

ОБЪЕДИНЕННЫЙ
ИНСТИТУТ
ЯДЕРНЫХ
ИССЛЕДОВАНИЙ

ДУБНА



4/7-77

A-29

E2 - 10471

2446/2-77

A.A.Akhundov, D.Yu.Bardin, N.M.Shumeiko

**ELECTROMAGNETIC CORRECTIONS
TO THE DEEP INELASTIC μp -SCATTERING
AT HIGH ENERGIES**

1977

E2 - 10471

A.A.Akhundov,¹ D.Yu.Bardin, N.M.Shumeiko²

**ELECTROMAGNETIC CORRECTIONS
TO THE DEEP INELASTIC μp -SCATTERING
AT HIGH ENERGIES**

Submitted to ЯФ

¹Azerbaijan State University, Baku.

²Byelorussian State University, Minsk.

Ахундов А.А., Бардин Д.Ю., Шумейко Н.М.

E2 - 10471

Электромагнитные поправки к глубоконеупругому μp -рассеянию при высоких энергиях

Вычислены электромагнитные поправки к глубоконеупругому μp -рассеянию при энергиях мюона $E = 50-250$ ГэВ. Для структурных функций использованы новейшие результаты анализа мировых данных по электро-рождению адронов в резонансной и глубоконеупругой областях ($E < 20$ ГэВ) с последующей экстраполяцией в область высоких энергий.

Найдено, что в большей части кинематической области поправки не чувствительны к выбору подгонки структурных функций.

Работа выполнена в Лаборатории теоретической физики ОИЯИ.

Препринт Объединенного института ядерных исследований. Дубна 1977

Akhundov A.A., Bardin D.Yu.,
Shumeiko N.M.

E2 - 10471

Electromagnetic Corrections to the Deep
Inelastic μp -Scattering at High Energies

The electromagnetic corrections are calculated to the deep inelastic μp -scattering at muon energy $E = 50-250$ GeV. The structure functions are found by using the latest results of analysis of the presently available data on hadron electroproduction in resonance and deep inelastic region ($E < 20$ GeV) with the subsequent extrapolation to high energies.

It is shown that in a large kinematical region the corrections are not sensitive to the fit of structure functions.

The investigation has been performed at the Laboratory of Theoretical Physics, JINR.

Preprint of the Joint Institute for Nuclear Research. Dubna 1977

1. INTRODUCTION

In view of the planned experiments on deep inelastic lepton-nucleon scattering at high energies ^{/1/} we investigate the electromagnetic corrections (EC) to this process.

The deep inelastic ℓN -scattering provides basic information on the nucleon structure defined by the structure functions W_1 and W_2 . In determining these functions from experimental data one faces with the problem of separation of the cross section of the process

$$\ell + N \rightarrow \ell + \text{hadrons} \quad (1)$$

in the Born approximation (diagram in Fig. 1) from the measured cross section of the inclusive process

$$\ell + N \rightarrow \ell + X, \quad (2)$$

where X is anything including hadrons, γ -quanta and additional leptons. To this end it is necessary to calculate and subtract from the observed cross section those process contributions which simulate the deep

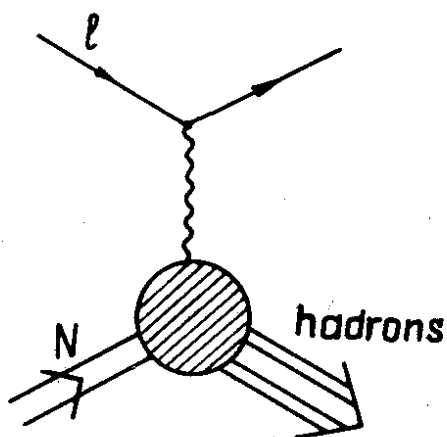


Fig. 1. Diagram of the deep inelastic eN -scattering in the one-photon approximation.

inelastic scattering but are not described by the diagram in Fig. 1. These processes are clearly described by diagrams of another than α order.

In the lowest α order this contribution can be represented as follows:

$$2\text{Re} \left[\begin{array}{c} \text{Diagram 1} \\ \text{Diagram 2} \\ \text{Diagram 3} \\ \text{Diagram 4} \end{array} \right] + \text{Diagram 5} + \text{Diagram 6} + \text{Diagram 7} \quad (3)$$

Figure (3) comprises the following EC:

- i) to the lepton current (diagrams 1,5,6),
- ii) from the vacuum polarization by electron and muon (diagram 2),
- iii) to the hadron current (diagrams 3 and 7),
- iv) from the two-phonon exchange (diagram 4) and from the interference of diagram 7 with diagrams 5 and 6.

Note that in the α^3 -order to the measured cross section a contribution comes also from the diagrams of vacuum polarization by hadrons. As is shown in paper /2/, in the range of transfer momentum Q^2 from 0 to 100 GeV^2 this contribution increases from 0 till 3%.

The hadron EC, i.e., iii) and iv) can be calculated only within a model. The analysis of all experiments on deep inelastic \mathbb{N} -scattering till now performed was made by assuming these corrections to be small. This assumption is supported by the parton model calculations /3/ of EC where it is shown that up to 250 GeV initial energy the hadron EC do not exceed $\pm 3\%$ in a large kinematic region.

The lepton EC, i.e., i) and ii) which can be found in a model independent way, have been calculated in the classical paper by L.W.Mo and Y.S.Tsai /4/. All the calculations of EC in performed experiments are essentially based on that paper. Since the lepton EC are relatively large (they amount to dozens of per cent), it is important to take thoroughly account just of their contribution.

In papers ^{/5,6/} and in the present paper we make an additional study of the lepton EC. We consider, it is necessary for the following reasons:

1. Some experiments on μp -scattering ^{/7/} are carried out in the region $Q^2 \approx m_\mu^2$ (m_μ - the muon mass). The formulae of Mo and Tsai are inapplicable at such Q^2 , therefore exact formulae are required.

2. Expressions for the EC in ref. ^{/4/} include the "softness" parameter Δ dividing the contributions of soft and hard photons thus breaking their Lorentz-invariance. However, in inclusive processes these contributions are not separated physically ^{/8/} therefore it would be reasonable to obtain formulae independent of the "softness" parameter and covariant in order to make them be applicable directly to the planned experiments on the colliding $e p(\mu p)$ beams.

In papers ^{/5,6/} exact Lorentz-invariant formulae are obtained for the contribution of the elastic radiative tail to the measured cross section and for the EC to the continuous spectrum valid throughout the whole kinematic region of deep inelastic eN -scattering. The radiative tail of the elastic peak was calculated by using the experimental fit of the proton form factors in the Q^2 -range up to 25 GeV^2 ^{/9/}, while the EC to the continuous spectrum by fitting the data on electron production within a parton model ^{/10/}.

In the present paper we make a more realistic calculation of the EC to the continuous spectrum. In the resonance region the structure functions are found on the

basis of the analysis of all existing data performed in paper /11/, whereas in the deep inelastic region $W > 2$ GeV the fit is used from paper /12/. We also examine the sensitivity of the EC to the fit of the structure functions. The next section discusses the results of calculation of the EC to the continuous spectrum by formulae listed in the Appendix.

2. DISCUSSION OF RESULTS

The calculation of the EC is directly related to the analysis of data of a specific experiment. Thus, to calculate the EC at some point $F(W^2, Q^2)$ of the kinematical region of the deep inelastic eN -scattering (Fig. 2), it is necessary to know the behaviour of structure functions inside triangle CFD (see (A.9) in the Appendix). To establish the structure functions from experimental data, the EC, in turn, should be calculated. Therefore, an iteration procedure is needed.

Before a new experiment will be performed, the EC can be evaluated by using information from previous experiments.

Figure 2 shows the region thoroughly investigated in SLAC and DESY experiments on ep -scattering.

To estimate the structure functions in the unexplored region, we extrapolate the recent data on electron production of paper /12/ into that region. The arguments in favour of this extrapolation are as follows.

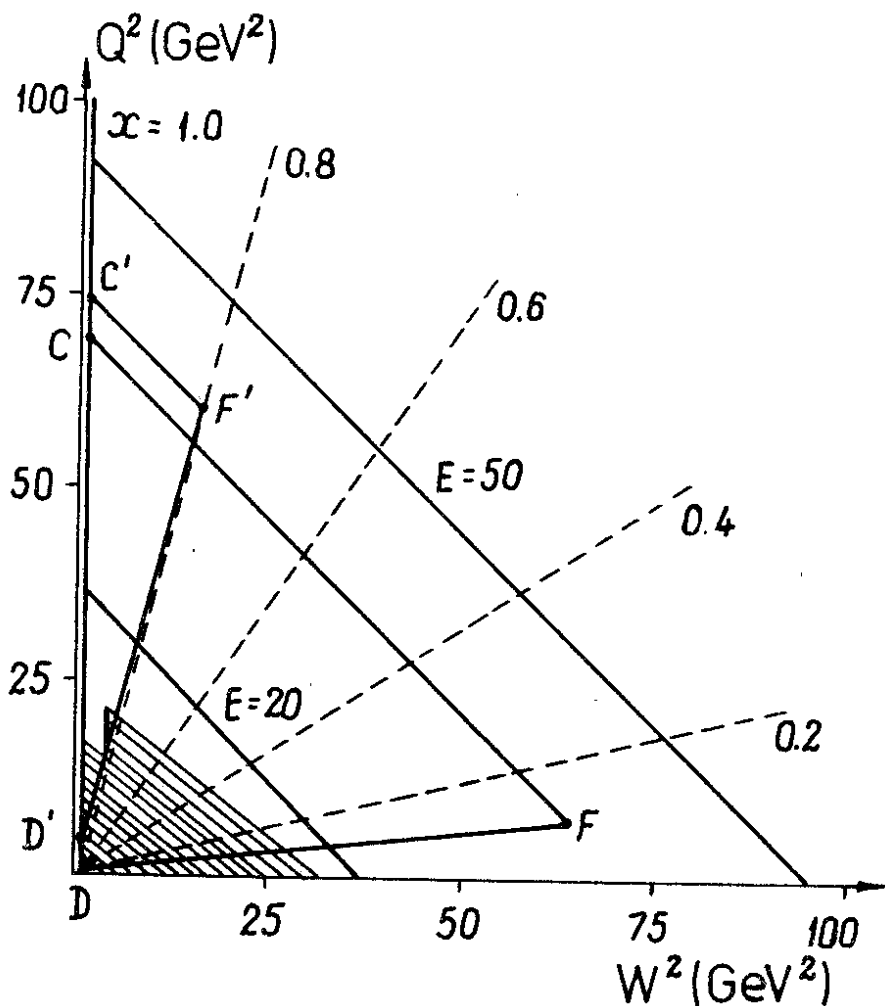


Fig.2. The kinematic region of the deep inelastic \mathbb{N} -scattering in the (W^2, Q^2) plane. The boundary is shown at $E=20$ and 50 GeV. Dotted lines correspond to x constant. The shaded region shows where the structure functions are studied in detail^{13/}. At $E=50$ GeV the triangles CFD and $C'F'D'$ denote the integration range in (A.9) for points $F(x=0.1, y=0.75)$ and $F'(x=0.8, y=0.8)$.

The fit in paper /12/ is obtained from the analysis of data in the range $2 < W < 5$ GeV, $0 < Q^2 < 2$ GeV². The extrapolation of this fit to large W at small Q² is in satisfactory agreement with the recent experimental data of FNAL on μp -scattering at E = 150 GeV /7/, and its extrapolation into the whole shaded region (in Fig. 2) agrees with the fit of the presently available data in that region at $Q^2 > 0.5$ GeV² (eqs. (38)-(40) of ref. /14/).

In another experiment of FNAL /15/ the observed cross section was compared with that expected. To calculate the latter the structure functions measured in SLAC were employed. The measured and calculated cross sections agree within to 20%.

However, our calculations show that if the EC are evaluated by using the fitting of the electron production data from ref. /10/, which produces the values of structure functions different even by a factor of two from those of ref. /12/, then the difference in the calculated EC is small in a large kinematic region.

The structure functions in the range of prominent resonances ($W < 2$ GeV, $Q^2 < 6$ GeV²) were calculated from the total cross section of the virtual photon absorption Σ given by eq. (3) of ref. /11/ (for $R = \sigma_L / \sigma_T$ it was put $R=0$ in the region $W < 1.6$ GeV, $Q^2 < 2$ GeV² and $R=0.18$ in the other part of the resonance region).

An effect of the choice of R was investigated on the contribution of the radiative tail from the resonance region. Setting $R=0$ or $R=0.18$ throughout the whole region, we

have found that this contribution changes not larger than by 10%. Since the contribution of the resonance tail amounts not larger than half of the total EC, which generally does not exceed 30%, inaccuracy in the absolute value of the total EC due to possible variation of R does not exceed 1%.

In the remaining region ($W < 2$ GeV, $Q^2 > 6$ GeV² and $W > 2$ GeV) the structure functions were found by eqs. (13), (14), (18) and (19) of paper^{/12/} at $R=0.18$. Thus, also in the region $W < 2$ GeV, $Q^2 > 6$ GeV² we made use of the fit obtained from the data analysis in the deep inelastic region only. The calculations show that the contribution of the radiative tail from the region $W < 2$ GeV, $Q^2 > 6$ GeV² is very small in a large kinematical region.

The calculated lepton EC to the cross section of the process

$$\mu + p \rightarrow \mu + \text{hadrons} \quad (4)$$

in the deep inelastic region $W > 2$ GeV by using the fits of refs. ^{/11,12/} are plotted in Figs. 3,4, where

$$\delta(x,y) \equiv \left(\frac{d^2\sigma_R}{dx dy} + \frac{d^2\sigma_V}{dx dy} \right) / \frac{d^2\sigma_0}{dx dy}, \quad (5)$$

$d^2\sigma_R/dx dy$ and $d^2\sigma_V/dx dy$ correspond to the contribution to the measured cross section from diagrams 5,6 and 1,2 of exp.3, resp. (x and y are the usual scaling va-

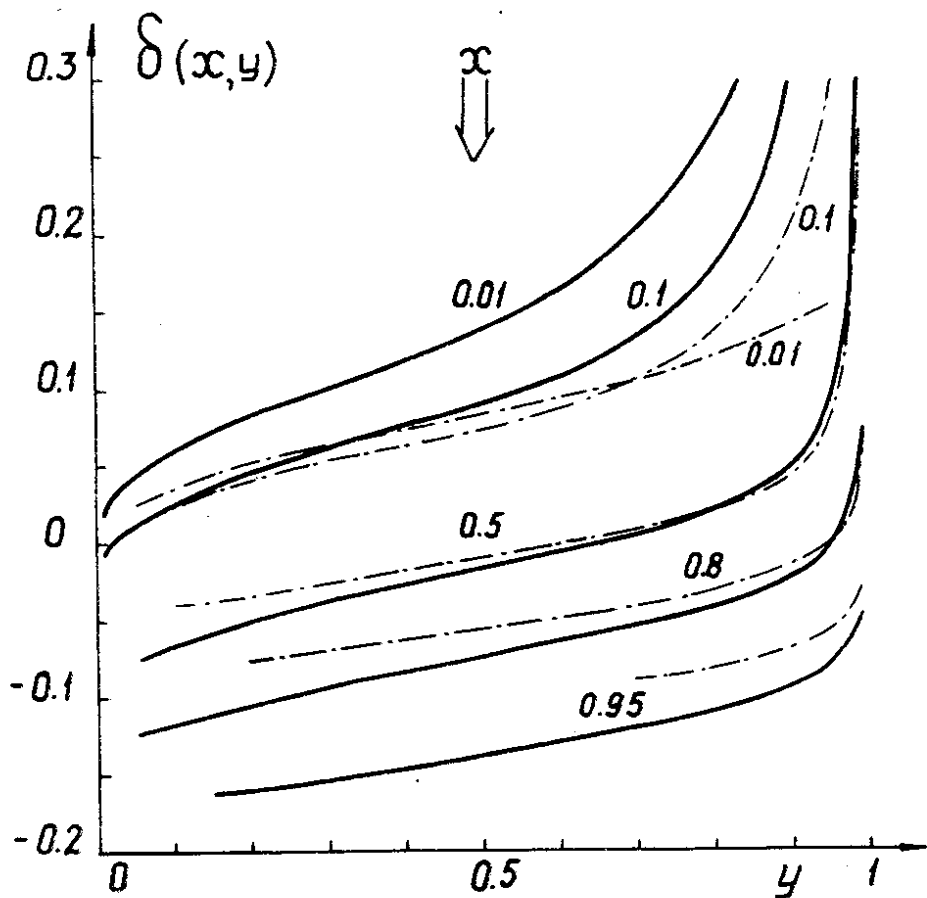


Fig. 3. Electromagnetic corrections to the cross section of the process $\mu + p \rightarrow \mu +$ hadrons at $E = 50$ GeV (dash-dotted lines) and at $E = 250$ GeV (solid lines).

riables) and $d^2\sigma_0/dx dy$ is the inclusive cross section of process (4) in the Born approximation.

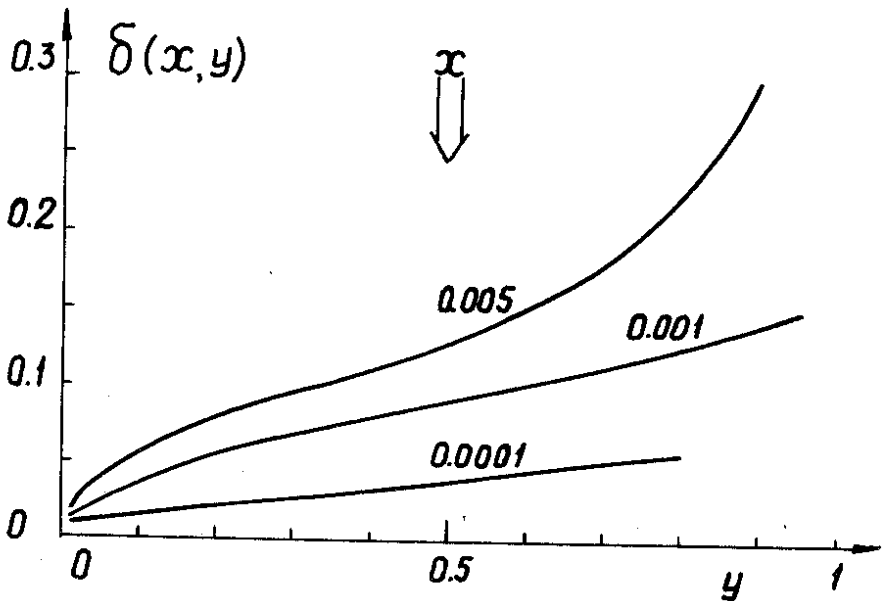


Fig. 4. Electromagnetic corrections to the process $\mu + p \rightarrow \mu + \text{hadrons}$ for small x ($E = 250$ GeV).

As is seen from the Figures, in a broad energy interval (50-250 GeV) the EC changes from -0.2 at $x \sim 1$ up to a large positive value at small x . However, with further decreasing x the EC starts to decrease. For instance, at $E = 250$ GeV this occurs at $x \sim 0.01$, and at $E = 50$ GeV - at $x \sim 0.1$. With increasing energy E modulo $\delta(x,y)$ increases at fixed x and y (see Fig. 3).

Note that like in paper ^{16/} we do not present the EC in the region x and y , where

$$|\delta(x,y)| > 0.3.$$

This region is forbidden for experiment in the sense that if the lower order EC are large also the higher order EC cannot be neglected. As is seen from Figures 3 and 4 this region is very narrow near $y = 1$, which is almost inaccessible for experiment. Nevertheless, it seems important to calculate the next order EC both for estimating the calculation accuracy and for theoretical investigation of higher order EC ^{/16/}.

The comparison of the calculated EC by using the realistic fits with the calculation from paper ^{/6/} performed under more limiting assumption on the structure functions (see Fig. 4 of ref. ^{/6/}) reveals perfect agreement in the range of not very small x (up to $x \sim 0.1$ at $E = 250$ GeV).

On the basis of the fact that the EC are stable relative to the fit of structure functions in a large kinematic region of the deep inelastic scattering it may be concluded that the iteration procedure for evaluating the EC will require a small number of steps. This conclusion, probably, is not correct for small x ($x \leq 0.05$ at $E = 250$ GeV), where a considerable sensitivity of the EC to the fit is found.

Our formulae permit us to calculate EC for any structure functions. When there appear new fits, e.g., allowing for the results of analysis of μp -scattering data up to 150 GeV, these should be used for calculating EC at the first iteration step.

We inspect also the validity of formulae obtained in the so-called Peaking Approximation ^{/4/}. In calculations of EC to the continuous spectrum this approximation is valid to those regions where a weak sensi-

vity to the structure functions was observed. The latter apparently explains the validity of the approximation. The Peaking Approximation is not applicable for calculations of the contribution of the elastic radiative tail at high energies ^{/5/}.

APPENDIX

The inclusive spectrum of leptons in the process

$$\ell + N \rightarrow \ell + \gamma + \text{hadrons} \quad (\text{A.1})$$

can be written in the form *

$$\frac{d^2\sigma_R}{dx dy} = \frac{2\alpha^3}{\lambda_S} S^2 y \int dM_f^2 \int \frac{dt}{t^2} \mathcal{S}(M_f^2, t), \quad (\text{A.2})$$

where

$$\mathcal{S}(M_f^2, t) = 2MW_1(M_f^2, t) \mathcal{S}_1(M_f^2, t) + \nu_h W_2(M_f^2, t) \frac{1}{T} \mathcal{S}_2(M_f^2, t), \quad (\text{A.3})$$

and $\mathcal{S}_1(M_f^2, t)$ and $\mathcal{S}_2(M_f^2, t)$ are given by eq. (21) of ref. ^{/6/}. Integral in (A.2) runs over the range

$$(M + m_\pi)^2 \leq M_f^2 \leq W^2, \quad (\text{A.4})$$

$$t_{\max, \min} = \frac{1}{2W^2} [(W^2 - M_f^2)(S_X \pm \sqrt{\lambda_Y}) + 2M_f^2 Y].$$

*Notation are from ref. ^{/6/} and $Q^2 \equiv Y..$

Expression (A.2) gives the contribution of the radiative tail of the continuous spectrum (R-contribution) to the observed cross section of the deep inelastic scattering.

Integral (A.2) at point (W^2, Y) has the infrared divergence, however, just at this point the diagrams with virtual photon exchange give contribution (V-contribution). The sum $R + V$ is free of divergences.

Now we represent the cross section of process (A.1) in the form

$$\frac{d^2 \sigma_R}{dx dy} \equiv \frac{d^2 \sigma_R^F}{dx dy} + \frac{d^2 \sigma_R^{IR}}{dx dy}, \quad (A.5)$$

where $d^2 \sigma_R^{IR}/dx dy$ is the part which contains the infrared divergence, and $d^2 \sigma_R^F/dx dy$ is infrared free part.

The separation of the infrared divergent part of (A.2) by the method described in refs. /6,8/ results in the formula

$$\frac{d^2 \sigma_R^{IR}}{dx dy} = \frac{d^2 \sigma_0}{dx dy} \cdot \frac{\alpha}{\pi} \delta_R^{IR}, \quad (A.6)$$

where

$$\delta_R^{IR} = J_0 \ln \frac{W^2 - (M+m_\pi)^2}{\lambda \sqrt{W^2}} + \frac{1}{2} (S'L_S + X'L_X) + \quad (A.7)$$

$$+ S_\phi (Y + 2m^2, \lambda_m, a', b'),$$

$$L_{S'} = \frac{1}{\sqrt{\lambda_{S'}}} \ln \frac{S' + \sqrt{\lambda_{S'}}}{S' - \sqrt{\lambda_{S'}}}, \quad L_{X'} = \frac{1}{\sqrt{\lambda_{X'}}} \ln \frac{X' + \sqrt{\lambda_{X'}}}{X' - \sqrt{\lambda_{X'}}},$$

$$\lambda_{S'} \equiv \lambda(S', m^2, W^2), \quad \lambda_{X'} \equiv \lambda(X', m^2, W^2),$$

$$S' = S + M^2 + m^2, \quad X' = -X + M^2 + m^2, \quad (\text{A.8})$$

$$a' = \frac{1}{2W^2} [SX - M^2Y - W^2(Y + 4m^2)],$$

$$b' = \frac{1}{W^2} [Y(SX - M^2Y) - m^2\lambda_Y].$$

The part of the cross section free of the infrared divergence has the form

$$\frac{d^2\sigma_R^F}{dx dy} = \frac{2\alpha^3}{\lambda_S} S^2 Y \int_{(M+m)^2}^{W^2} dM_f^2 \int_{t_{\min}}^{t_{\max}} dt \left[\frac{1}{t^2} \mathcal{S}(M_f^2, t) - \frac{1}{Y^2} \mathcal{S}^{IR}(M_f^2, t) \right], \quad (\text{A.9})$$

where

$$\begin{aligned} \mathcal{S}^{IR}(M_f^2, t) &= \frac{1}{\pi} \int_{z_{\min}}^{z_{\max}} \frac{dz}{\sqrt{R_z}} \mathcal{S}^{IR} = 2MW_1(W^2, Y) \mathcal{S}_1^{IR}(M_f^2, t) + \\ &+ \nu \ell W_2(W^2, Y) \frac{1}{S_X} \mathcal{S}_2^{IR}(M_f^2, t), \end{aligned} \quad (\text{A.10})$$

$$\mathcal{S}_1^{IR}(M_f^2, t) = (Y - 2m^2) F^{IR}(M_f^2, t), \quad \mathcal{S}_2^{IR}(M_f^2, t) = 2(SX - M^2Y) F^{IR}(M_f^2, t),$$

$$F^{IR}(M_f^2, t) = \left\{ \frac{Y + 2m^2}{t - Y} \frac{1}{\sqrt{-C_z}} - m^2 \frac{B_z}{(-C_z)^{3/2}} \right\} - \{S \leftrightarrow X\} \quad (\text{A.10})$$

The formulae obtained for $d^2\sigma_R/dx dy$ together with those for V-contribution, $d^2\sigma_V/dx dy$, given in paper /6/ define completely the EC to the continuous spectrum.

REFERENCES

1. F.Krienen et al. CERN/SPSC/ 74-79, P19, 1974;
R.Cliff et al. CERN/SPSC/74-78, P18, 1974.
2. F.A.Berends, G.J.Komen. Phys.Lett., 63B, 432 (1976).
3. Д.Ю.Бардин, Н.М.Шумейко. ОИЯИ, P2-9940, Дубна, 1976.
4. L.W.Mo and Y.S.Tsai. Rev.Mod.Phys., 41, 205 (1969).
5. A.A.Akhundov, D.Yu.Bardin, N.M.Shumeiko. JINR, E2-10147, Dubna, 1976.
6. A.A.Akhundov, D.Yu.Bardin, N.M.Shumeiko. JINR, E2-10205, Dubna, 1976.
7. H.L.Anderson. Paper No. 252 contributed to the XVIII Int. Conf. on High Energy Physics, Tbilisi, 1976.
8. Д.Ю.Бардин, Н.М.Шумейко. ОИЯИ, P2-10113, Дубна, 1976.
9. С.И.Биленькая, С.М.Биленький, Ю.М.Казаринов, Л.И.Липидус. Письма в ЖЭТФ, 19, 613 (1974).
10. V.Barger, R.J.N.Phillips. Nucl.Phys., B73, 269 (1974).

11. F.W.Brasse et al. Nucl.Phys., B110, 413 (1976).
12. S.Stein et al. Phys.Rev., D12, 1884 (1975).
13. W.B.Atwood. SLAC Report-185, 1975.
14. S.I.Bilenkaya, S.M.Bilenky, Yu.M.Kazarinov, L.I.Lapidus. JINR, E1-7275, Dubna, 1973; ЖЭТФ, 65, 1745 (1973).
15. C.Chang et al. Phys.Rev.Lett., 35, 901 (1975);
Y.Watanabe et al. Phys.Rev.Lett., 35, 898 (1975).
16. L.C.Maximon. Rev.Mod.Phys., 41, 193 (1969).

Received by Publishing Department
on March 1, 1977.